

## BIOSYNTHESIZED SILVER NANOPARTICLES USING *CATHARANTHUS ROSEUS* AND THEIR ANTIBACTERIAL EFFICACY IN SYNERGY WITH ANTIBIOTICS; A FUTURE ADVANCEMENT IN NANOMEDICINE

MONIKA GUPTA\*

Amity Institute of Biotechnology, Amity University Madhya Pradesh, Gwalior, Madhya Pradesh, India.

Email: biotech.monikaphd@gmail.com

Received: 01 October 2020, Revised and Accepted: 09 January 2021

**ABSTRACT**

**Objective:** This research work develops an approach to synthesize silver nanoparticles (AgNPs) by reduction of leaf extract of *Catharanthus roseus* plant. This study produces synthesized nanoparticles that have process-controlled attributes which make their antibiotic action highly efficient. These attributes include smaller size, proper morphology, uniform dispersion, metal ion content, and formation of functional groups. By optimizing the reduction process parameters, AgNPs gain the desired properties.

**Methods:** The biosynthesis of AgNPs process was performed using reaction of 10% (w/v) *C. roseus* leaf extract with  $\text{AgNO}_3$ . The optimum conditions and concentration used for synthesis of nanoparticles were: 1 mM  $\text{AgNO}_3$ ,

pH 5, and temperature 80°C with an incubation time of 72 h. All the above parameters were analyzed by ultraviolet-visible spectrophotometer with the surface plasmon resonance peak obtained at 440 nm.

**Results:** Various characterization techniques were performed, namely, scanning electron microscopy, energy-dispersive X-ray, transmission electron microscopy, photoluminescence study, X-ray diffraction spectroscopy, Fourier transform infrared, dynamic light scattering, and atomic force microscopy. The results obtained from characterization confirmed the spherical morphology of the nanoparticles with size between 50 and 87 nm. In the current investigation, the antimicrobial activity of biosynthesized AgNPs was also determined using minimum inhibitory concentration and zone of inhibition methods against six different bacteria at different doses of AgNPs (100, 150, and 200 µg/ml) alone and also in combination with antibiotic-streptomycin.

**Conclusion:** The results revealed that high concentration of AgNPs inhibits the bacterial growth. Furthermore, AgNPs revealed much stronger antibacterial action in synergy with streptomycin against antibiotic-resistant bacteria.

**Keywords:** Biosynthesis, Physical parameters, Ultraviolet-visible spectroscopy, Characterization, Antimicrobial activity.

© 2021 The Authors. Published by Innovare Academic Sciences Pvt Ltd. This is an open access article under the CC BY license (<http://creativecommons.org/licenses/by/4.0/>) DOI: <http://dx.doi.org/10.22159/ajpcr.2021v14i2.39856>. Journal homepage: <https://innovareacademics.in/journals/index.php/ajpcr>

**INTRODUCTION**

The role of green nanoparticles has gained prominence as a result of substantial increase in their application in biosensors, bio-nanotechnology, biomedicine, etc. [1]. Various physical and chemical methods are also used for synthesizing nanoparticles but these are costly and require extensive labor and time. Furthermore, these methods generate large amounts of secondary wastes due to use of hazardous chemical reagents during reduction process. Thus, there is a growing demand for an alternate process. Biological synthesis of nanoparticles is a much rapid, economically feasible, and eco-friendly process. It gives nanoparticles of desired morphology and size.

In recent times, biological materials such as plants are used as an efficient method to synthesize nanoparticles. Examples include such as silver nanoparticles (AgNPs) from banana peel extract [2], Neem leaves [3], etc.

AgNPs have been widely used in biomedical and healthcare industry and have various applications in subfields of nano-medicine such as diagnostics, nano-electronics, and molecular imaging. These are also used as anticancer, antifungal, anti-inflammatory, wound healing, and antibacterial agents due to their cytotoxic nature [4-8].

This study is an endeavor to synthesize green AgNPs using leaf extract of *Catharanthus roseus* plant, a source of more than 200 alkaloids. Every part of this plant contains various alkaloids, phenolics, terpenoids, and glycosides which are used for the treatment of diabetes, cancer, malaria, menorrhagia, etc. Due to the presence of several secondary metabolites including ajmalicine, vinblastine, serpentine, phenolic compounds, and vincristine, it is considered as a highly valuable medicinal plant. The metabolites present in *C. roseus* act as reducing and capping agents. These help in binding and reducing metal ions and providing stability during the formation of nanoparticles.

The effect of various physiochemical parameters (pH, temperature, metal ion concentration, and incubation time) was analyzed to procure optimum attributes of synthesized nanoparticles which would render high anti-bacterial efficacy of nanoparticles. Various characterization techniques have been used for evaluating the features of synthesized nanoparticles.

The AgNPs with controlled structures that are uniform in size and shape and morphology have successful antibacterial applications. Very tiny AgNPs (nanometer range) are capable of rupturing the cell wall and entering into microbial cells which leads to cell death. Thus, AgNPs may overcome limitations of existing antibiotics by combating multi-drug resistant bacteria.

Antibacterial effect of the synthesized AgNPs has also been explored in this research against six bacteria with AgNPs alone and in synergy with an antibiotic.

A major benefit that this study renders is formation of nanoparticles which can act as highly potent antibiotic through *C. roseus* plant which is available in all season. Hence, there would be no dearth of raw material supply. Second, no harmful reagents are used and the method developed is simple, feasible, cheap, and very convenient to perform.

The results of this study can further produce a highly potent antibacterial drug which can produce much better results than antibiotic (when used alone) and to combat antibiotic-resistant bacteria.

**MATERIALS AND METHODS****Materials**

*C. roseus* leaves were collected from Gwalior, India and washed with tap water then shade dried at 25°C, followed by grinding into fine powder.

Silver nitrate ( $\text{AgNO}_3$ , 99.9%) was purchased from Thermo Fisher Scientific India Pvt. Ltd. (Mumbai).

#### Preparation of *C. roseus* extract

The dried leaf powder (10 g) was dissolved in sterilized autoclaved water (100 ml) and stirred overnight. The leaf extract was filtered and was centrifuged at 3000 rpm for 20 min at room temperature; the supernatant was collected for further processing of biosynthesis of AgNPs. The remaining part of the supernatant was stored at 4°C.

#### Biosynthesis of AgNPs

To synthesize AgNPs, 10 ml of the extract was added to a beaker containing 90 ml of  $\text{AgNO}_3$  (1 mM) [9], then the mixture was heated at 80°C for 30 min. After 30 min, solution turned from yellowish color to a dark reddish-brown color (Fig. 1) which marked the formation of AgNPs [10,11]. Intermediate compounds at 0 h and 24 h were formed during the reduction reaction (Fig. 1). Reduction reaction can be indicated as:



Plant leaf contains high level of poly-phenols (Flavonoids) which contains hydroxyl and ketonic groups that reduce the metal salt. Leaf extract releases flavonoids into the  $\text{AgNO}_3$  solution in which  $\text{Ag}^+$  ions combine with flavonoids to form substrate complex and form protein capped AgNPs (Fig 1).

#### Factors influencing synthesized AgNPs

The effect of various physical and chemical factors parameters, which play an important role in the synthesis of nanoparticles of desired attributes, was studied through a double beam ultraviolet (UV)-visible spectrophotometer.

#### pH

The pH was adjusted using 0.1 M HCl and 0.1M NaOH, and maintained at 5, 7, 9, and 11 for the duration of reaction time. The metal salt concentration and temperature of 80°C were kept constant.

#### Temperature

The temperature of the synthesis process was maintained at 30°C, 50°C, and 80°C using a water bath, while the volume (10 ml) of the leaf extract and the metal ion concentration were kept constant.

#### Metal ion concentration

The concentration of Ag ion was maintained at different concentrations 0.1, 0.5, 1.0, and 10 mM. Metal ion concentration was constant and temperature and pH was maintained at 80°C and pH 5, respectively.

#### Incubation time

The nanoparticle solution was incubated at different times: 0 h, 12 h, 24 h, and 72 h.

#### Characterization of AgNPs

##### UV-visible spectra analysis

The absorbance of the AgNPs was recorded using a spectrophotometer (Shimadzu UV-2450, Japan) in the range of 300–600 nm.

##### X-ray diffraction spectroscopy (XRD) analysis

An X-ray diffract meter operated at 40 kV and 30 mA and at  $2\theta$  angle pattern with scanning range of 20°–80° (Model-Rigaku-miniFlex600) is used and their size is determined by the Debye-Scherrer equation  $D = 0.9 \lambda / \beta \cos\theta$

##### Fourier transform infrared (FTIR) analysis

For the FTIR analysis, the dried powder sample was prepared by mixing purified nanoparticles with potassium bromide (KBr) (10 mg), and again dried to remove the moisture content, after which the FTIR characterization was performed using Perkin-Elmer FTIR-105627, USA [12].

##### Dynamic light scattering (DLS) analysis

Five hundred microliters of nanoparticles solution diluted with 3 ml of sterilized distilled water were poured into the zeta dip cell and measured by intensity versus time graph which gives the polydispersity

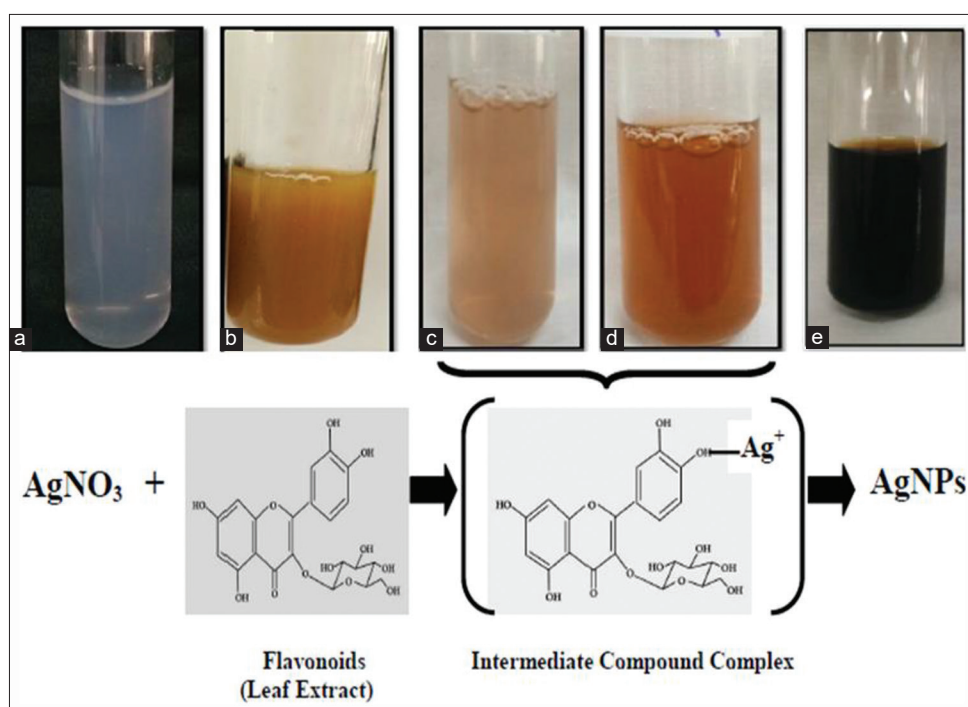


Fig. 1: Sequential color change due to intermediates formed at different time intervals in reduction reaction by 1 mM silver nitrate during the synthesis of silver nanoparticles: (a) Silver nitrate; (b) leaf extract; (c) 0 h; (d) 24 h; (e) 72 h

index (size distribution profile) of zinc oxide (ZnO) NPs. (Instrument: Nano plus – Zetasizer).

#### Photoluminescence analysis

The photoluminescence property of the nanoparticles was characterized using an eclipse fluorescence spectrophotometer (Model-Shimadzu RF-5301 PC). The nanoparticles exhibited visible photoluminescence in the fluorescence spectra. The green synthesized nanoparticles were found to be luminescent with two emissions and an excitation.

#### Atomic force microscopy (AFM) analysis

A thin film of the colloidal solution of AgNPs was prepared on a glass substrate (glass slide). The solution was allowed to dry on glass slide for 15 min and then scanned with the AFM (NT-MDT, Russia).

#### Scanning electron microscopy (SEM), energy-dispersive X-ray (EDX), and transmission electron microscopy (TEM) analysis

A thin film of the colloidal solution of AgNPs was prepared on a carbon coated copper grid substrate by placing few drops of the solution on the grid and allowed to dry under a mercury lamp for 10 min and was further characterized using SEM-EDX and TEM.

#### Measuring Anti-bacterial activity

Anti-bacterial activity of AgNPs was determined against Gram-positive and Gram-negative bacteria using minimum inhibitory concentration (MIC) method [13] and calculation of zone of inhibition (ZOI). Gram-positive bacterial strains were *Staphylococcus aureus* MTCC 9760, *Bacillus megaterium* ATCC® 14581, and *Streptococcus pyogenes* MTCC 1926 while *Proteus mirabilis* MTCC 3310, *Pseudomonas aeruginosa* MTCC 424, and *E. coli* MTCC 40 were the Gram-negative strains.

One milliliter bacterial sample was inoculated in 9 ml MHB. Then, it was serially diluted from  $10^{-1}$  to  $10^{-6}$  CFU/ml. Bacterial concentration from

each test tube ( $10^{-1}$ – $10^{-6}$  CFU/ml) was spread on MHA and kept for 24 h and  $37^{\circ}\text{C}$  in BOD and subjected to plate count method [14]. After 24 h, colonies of bacteria were counted through colony counter meter. Comparing the bacterial counts of  $10^{-1}$ – $10^{-6}$ , the minimum bacterial concentration was found in  $10^{-6}$  CFU/ml. Hence,  $10^{-6}$  CFU/ml is the subsequent MIC which would be taken to determine ZOI in the next step. MIC was determined one by one for each of the six bacteria.

Bacterial concentration of  $10^{-6}$  CFU/ml spread on MHA is the blank control Fig. 2a. Then, Whatman filter paper no. 1 disks of AgNPs having different concentrations: 100  $\mu\text{g/ml}$ , 150  $\mu\text{g/ml}$ , and 200  $\mu\text{g/ml}$  were placed on MHA without streptomycin Fig. 2b-d.

Again, different disks were prepared with 10  $\mu\text{g/ml}$  streptomycin with varying concentrations of AgNPs: 100  $\mu\text{g/ml}$ , 150  $\mu\text{g/ml}$ , and 200  $\mu\text{g/ml}$  were placed on MHA Fig. 2e. After keeping for 24 h and at  $37^{\circ}\text{C}$ , the synergistic antibacterial activity of AgNPs with streptomycin was measured in terms of ZOI.

## RESULTS AND DISCUSSION

### Effect of physicochemical parameters on properties of AgNPs by UV-visible analysis

#### Effect of pH

Changing the pH affects the size and morphology of the nanoparticles because the pH has the ability to modify the charge of the biomolecules. In the present study, observation peak was observed at pH of 5. The surface plasmon resonance absorption wavelength was measured at 425 nm which matches the surface plasmon resonance (SPR) band wavelength of 420–440 nm for AgNPs. At lower pH, the bioavailability of functional groups in *C. roseus* leaf extract promotes the synthesis of nanoparticles. However, in case of very low pH 0–3, no observation peak was observed due to inactivity of biological groups [15]. Moreover, it was observed that at alkaline pH, that is,  $\text{pH} > 7$ , the formation of nanoparticles was suppressed and at very high pH, that is,  $\text{pH} \sim 11$ ,

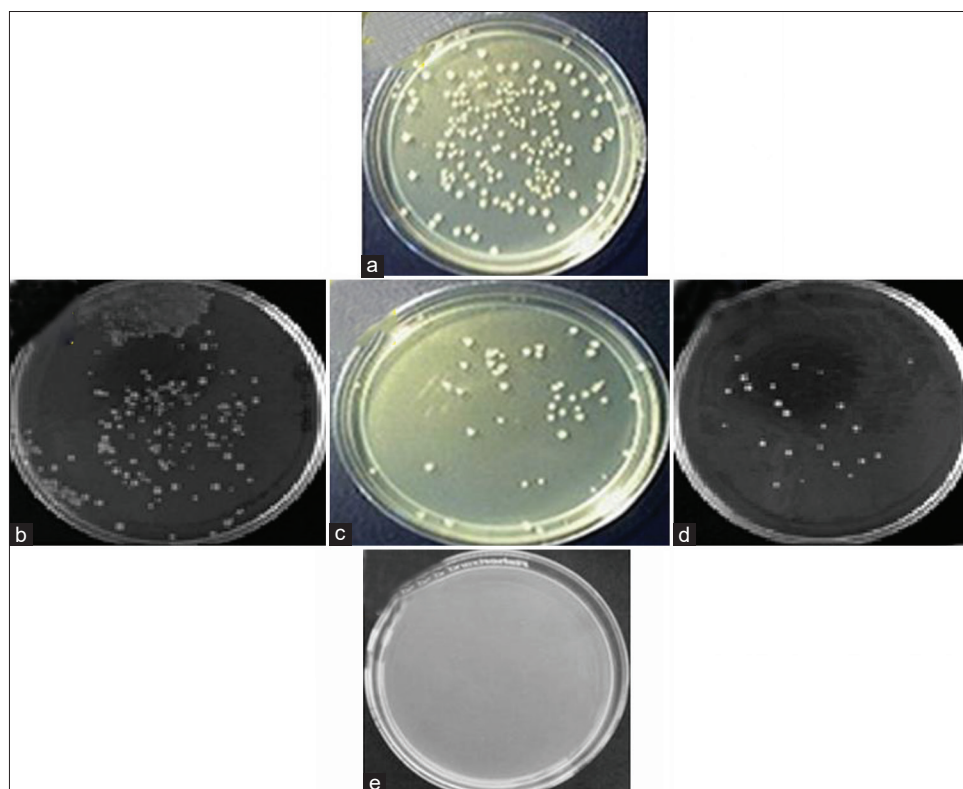


**Fig. 2:** Bacterial colonies count in MHA during antibacterial tests: (a): Blank control: Minimum inhibitory concentration  $10^{-6}$  CFU/ml; (b): Silver nanoparticles (AgNPs) alone at 100  $\mu\text{g/ml}$ ; (c): AgNPs alone at 150  $\mu\text{g/ml}$ ; (d): AgNPs alone at 200  $\mu\text{g/ml}$ ; (e): AgNPs with streptomycin at 200  $\mu\text{g/ml}$

the particles become unstable and agglomerated when kept overnight. The size and morphology of synthesized nanoparticles can thus be controlled by changing the pH of the bio-reduction process (Fig. 3a).

#### Effect of temperature

Synthesis of nanoparticles was performed at three different temperatures (30, 50, and 80°C). The absorption peak was obtained at 80°C (435 nm: lying in the SPR range), which is due to the localization of the SPR of the AgNPs. Similar results were also reported by Prasad and Elumalai [16] in leaf extract of *Moringa oleifera* at 80°C. At lower temperature (30°C and 50°C), no sharp band was found Fig. 3b but at very high temperature, the reduction occurred very hastily [17].

#### Effect of metal ion concentration

Different concentrations (0.1, 0.5, 1.0, and 10 mM) of AgNO<sub>3</sub> were used for the synthesis of nanoparticles. The maximum peak intensity obtained at 1 mM of AgNO<sub>3</sub> was 435 nm (lying in the SPR band) and spherical nanoparticles were formed Fig. 3c. A decrease in metal ion concentration has the ability to modify the particle size and morphology of nanoparticles whereas very high metal ion concentration changed the morphology to triangular, hexagonal, radial, and rod-shaped nanoparticles instead of spherical. A study on neem leaf extract, banana peel, and *Jatropha curcas* reported similar changes in the morphology and size of the nanoparticles during the synthesis of AgNPs due to change in salt concentration [2,18].

#### Effect of incubation time

In the present study, different incubation time periods (0, 12, 24, and 72 h) were tested. The characteristic absorption peak was observed at 440 nm at an incubation time of 72 h. No other sharp band was reported at 0–24 h (Fig. 3d). The incubation time depends on the nature of metals also. For AgNPs, the minimum incubation time required is 72 h for the complete reduction of metal ions. Similar results were also obtained in the biosynthesis of AgNPs from leaf extract of *Vitex negundo* [19].

#### FTIR analysis

Functional groups present in *C. roseus* leaf extract and AgNPs were characterized by FTIR spectroscopy. The spectrum showed several

peaks which indicated the complex nature of the bio-material. The bands observed in the FTIR spectrum during the biosynthesis of AgNPs using *C. roseus* leaf extract were 3369, 2924, 1638, 1400, 1046, and 560 cm<sup>-1</sup>. Due to the presence of functional groups, sharp peaks were observed for the synthesized AgNPs [20]. The broad peak obtained at 3369 corresponded to O-H, stretching H bonded strong band, the peak at 2924 corresponded to C≡H (stretch) strong alkane group. Furthermore, 1638 cm<sup>-1</sup> represents a C=C stretching the variable alkenes group present. C=C aromatic or C-F of alkyl halide and ether C-O or ester bonded at 1400 and 1046 cm<sup>-1</sup>, respectively Table 1. The shift in transmittance bands of leaf extract indicates the participation of biological functional groups (flavonoids, proteins, sucrose, and amines) from leaf extract to synthesize AgNPs [21]. FTIR spectra peak indicated that the high intensity sharp band around 3500 cm<sup>-1</sup> was due to the stretching (Fig. 4a) mode of Ag with metal salts through the functional groups which mediate the reduction reaction and act as capping agents to form AgNPs and stabilize them [22].

#### XRD analysis

To verify the results obtained from the UV-visible spectral analysis, *C. roseus* leaf extract was examined by XRD. The crystalline nature and size of AgNPs were determined from Bragg's reflection peaks observed in the XRD pattern Fig. 4b. The broadening of the peaks indicates the formation of AgNPs within the nanometer range. For AgNPs, the Bragg's reflections peaks were located at 2θ value of 32.39°, 38.32°, 46.37°, 67.58°, and 77.58° corresponding to (100), (111), (200), (220), and (311)

Table 1: Functional groups present in synthesized AgNPs

S. No.	Absorption peak (cm <sup>-1</sup> ) in AgNPs	Bond/functional groups
1.	3369	O-H stretch H- bonded strong bond
2.	2924	-C≡H (stretch) strong alkenes
3.	1638	-C=C-stretch variable alkenes
4.	1400	Alkenes -C-H
5.	1046	Alkyl halide C-F
6.	560	Alkyl halide C-F

AgNPs: Silver nanoparticles

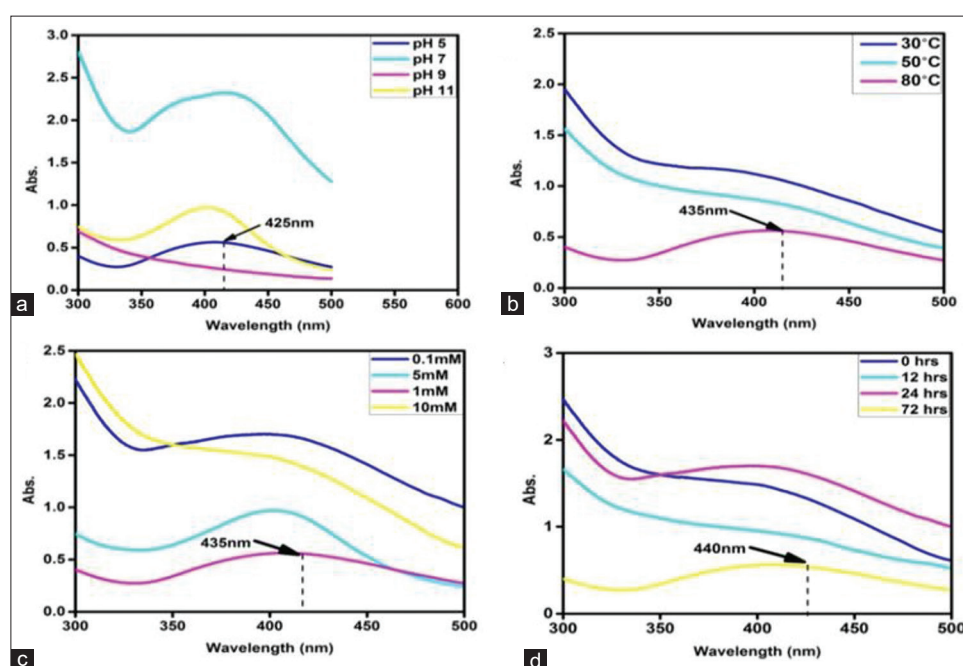


Fig. 3: (a) Effect of pH (b) effect of temperature (c) effect of concentration of metal ion (d) effect of reaction time on biosynthesis of silver nanoparticles

lattice planes, respectively. The similar XRD pattern was also obtained in banana and *Aloe vera* [2,23]. All the main peaks confirming the face cubic centered crystalline nature of the nanoparticles were shown in the standard data (JCPDS file No. 04-0783). The X-ray diffractions were recorded within the angle of 20°–80° and most of the diffraction peaks can be allocated to silver according to literature. The highest intensity peak at (111) plane of AgNPs with other smaller intensity peaks (110, 200, 211, 222, and 311) was observed. The particle size was calculated from the XRD pattern using Debye Scherrer's equation:

$$D = 0.9 \lambda / \beta \cos \theta$$

Where, D is the crystallite size for the (hkl) plane,  $\beta$  is FWHM in radiations,  $\lambda$  is the wavelength, and  $\theta$  is the X-ray diffraction angle for the (hkl) plane. The average AgNPs size was found to be 58.58 nm which was against the highest intensity peak at plane (111) Table 2. There was no impurity in XRD pattern which proved that pure AgNPs were synthesized. Our experimental spacing data matched with the calculated data.

### DLS analysis

The size distribution, polydispersity index (PDI) and the average size of the particles of the green synthesized ZnONPs were determined by DLS. The PDI was found to be 0.258 for AgNPs, which revealed the heterogeneity of the nanoparticle population (Fig. 5a). For AgNPs, PDI value >0.7 indicates polydispersed nature and larger size [24]. PDI = 0.258 proved that AgNPs were monodispersed and no agglomeration was found. The obtained results also revealed the size of AgNPs to be 50.3 nm.

### Photoluminescence study

The photoluminescence study was performed in order to discover the two essential peaks; the excitation and emission peak of the AgNPs [25]. This gives information about the band gap to excite electrons and crystalline purity of AgNPs. PL spectra of diluted AgNPs sample at room temperature showed the excitation at 283 nm and emission peaks at 566 nm Fig. 5b. The excitation spectrum was recorded from 280 to 500 nm while the emission was recorded from a wavelength of 500 to 750 nm. The peak originated at 558 nm by recombination which infers the possibility of AgNPs to show photoluminescence when pumped optically.

Table 2: The particle size and peak indexing of AgNPs

2 $\theta$ of the intense peak (deg)	$\theta$ of the intense peak (deg)	FWHM of intense peak ( $\beta$ ) in radian	Size of the particle(D) nm	d-spacing nm	(h k l)
32.39	16.19	0.0046	31.40 nm	0.2771 nm	100
38.32	19.16	0.0171	58.58 nm	0.234 nm	111
46.37	23.18	0.0056	26.98 nm	0.1960 nm	200
67.58	33.79	0.0055	30.34 nm	0.1385 nm	220
77.58	38.79	0.0257	06.92 nm	0.1230 nm	311

AgNPs: Silver nanoparticles

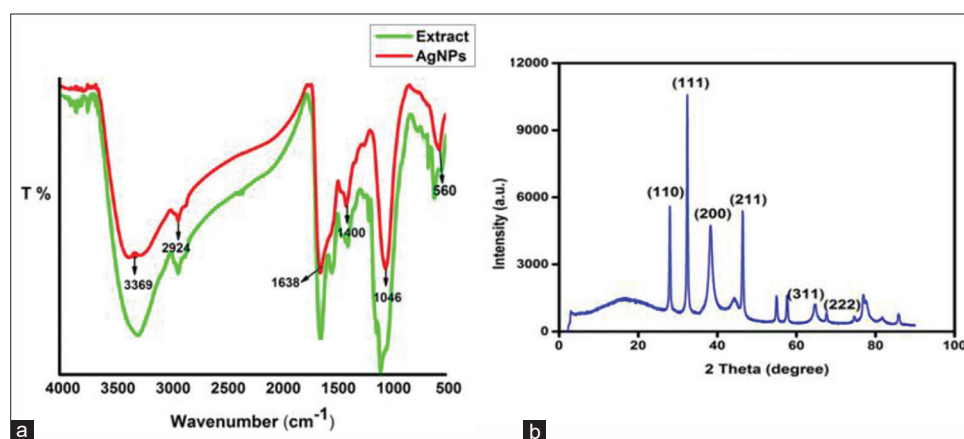


Fig. 4: (a) Fourier transform infrared (FTIR) spectra of biosynthesized silver nanoparticles (AgNPs) as compared to FTIR of leaf extract. (b) X-ray diffraction patterns of AgNPs

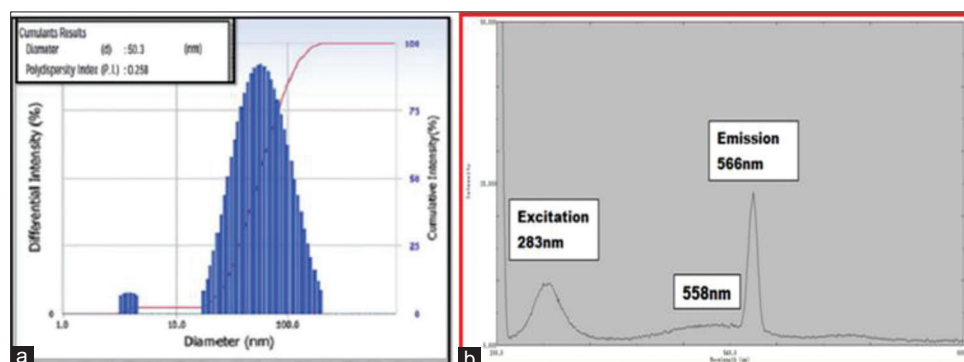


Fig. 5: (a). Dynamic light scattering analysis of silver nanoparticles (AgNPs). (b) Excitation and emission spectra of AgNPs

### AFM analysis

AFM analysis gives insight about the surface topography and roughness of AgNPs. The size of the AgNPs was obtained from the topography of the 3-D AFM image. It shows smooth nanoparticles along with capping of phytochemicals on the surface. The topography calculated for AgNPs, Fig. 6 was in the range of 50–60 nm. These results are similar to previous study carried out in *Clonorchis sinensis* [26]. Monodispersed AgNPs size observed by AFM line profile was 50 nm which was close to XRD results.

### SEM, EDAX and TEM analysis

SEM was used to observe the particle shape and size, surface morphology of the synthesized nanoparticles. The scanning electron microscope images of AgNPs showed Fig. 7a sizes ranging from 67 to 100 nm, with the presence of spherically shaped AgNPs. Similar results were observed for AgNPs prepared from *Insulin plant* and *A. vera* plants, [23,27]. However, in *A. vera*, spherical particles size were little bigger between 70.7 and 192.02 nm. Fig. 7b represents the EDAX analysis of AgNPs, showing the elemental composition of Ag and

chlorine (Cl) confirming formation of AgNPs and also the presence of metallic  $\text{AgNO}_3$  in the biosynthesized AgNPs. The EDAX analysis displays the optical absorption peaks of Ag and Cl resulting from the surface plasmon resonance of AgNPs.

The size and shape of the resultant particles were illuminating with the help of TEM Fig. 7c and d. The TEM micrograph suggests that the sizes of the particles were recorded 60 nm in spherical shape.

### Determination of antimicrobial activity by ZOI method

Previously, several studies reported that AgNPs synthesized from plants have prominent antibacterial activity [28-31]. Results show that 100  $\mu\text{g/ml}$  and 150  $\mu\text{g/ml}$  concentration of AgNPs were used, the bacterial concentration slightly decreased but when 200  $\mu\text{g/ml}$  concentration of AgNPs was used, the growth of six pathogens was inhibited to a great extent ZOI – Table 3 and Fig. 8. It was also observed that among the six bacteria, AgNPs were more active against *P. mirabilis* MTCC 3310: Gram-negative bacteria (12.58 mm ZOI) than *S. aureus* MTCC 9760: Gram-positive bacteria (11.11 mm ZOI). It can be concluded

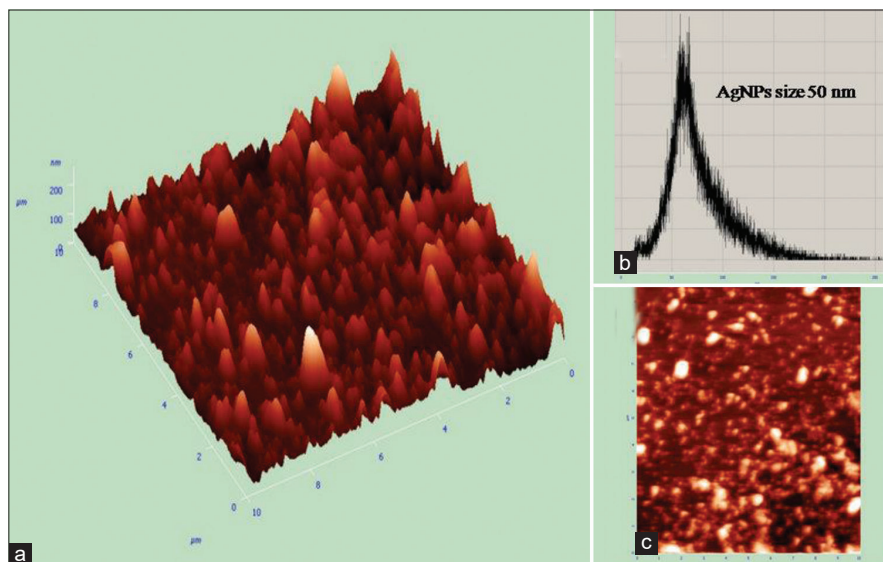


Fig. 6: Atomic force microscopy results of silver nanoparticles (a) 3D images (b) histogram graph (c) 2D images

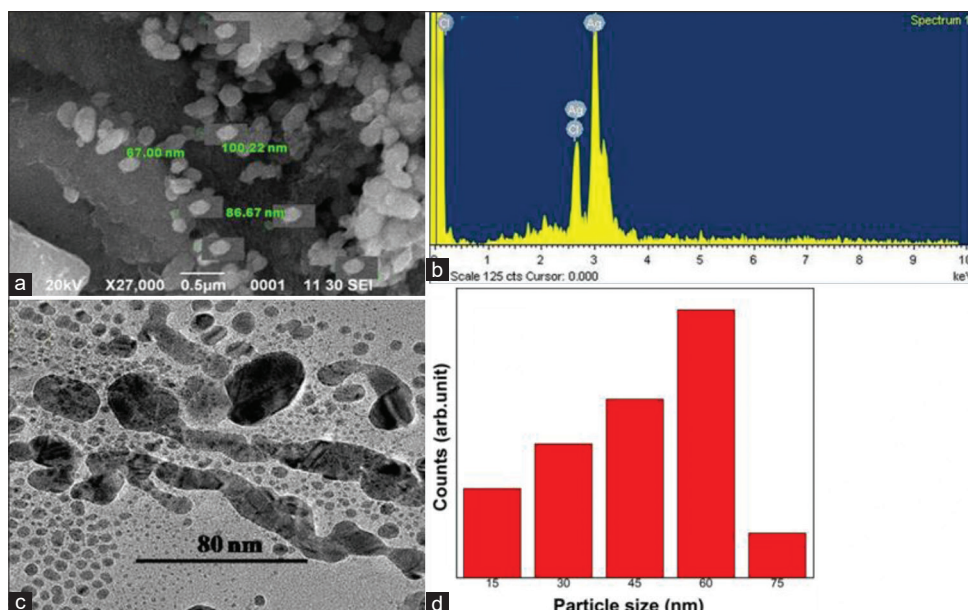


Fig. 7: (a) Scanning electron microscopy (SEM) images of the silver nanoparticles (AgNPs). The SEM images reveal size as 60 nm (b) energy-dispersive X-ray spectrum of the AgNPs (c) transmission electron microscopy image of the AgNPs (scale bar indicates 80 nm) (d) histogram of the size distribution of AgNPs

that AgNPs are bactericidal at high concentration but bacteriostatic at low concentration. Therefore, AgNPs synthesized in this study will be suitable for preventing pathogenic bacterial contamination [32].

#### Synergistic effect

Streptomycin (a standard antibiotic) taken 10 µg/ml and alone did not show very good activity against the six tested pathogens. However, the combined effect of streptomycin with AgNPs displayed a strong antibacterial activity against these six bacteria at 200 µg/ml concentration as compared to streptomycin combined with 100 µg/ml and 150 µg/ml with ZOI ranging from 13.60 to 15.30 mm (Table 3 and Fig. 8). The highest ZOI was obtained at

20 µg/ml concentration for Gram-negative bacteria as compared to Gram-positive bacteria.

#### Mechanism of antibacterial action of AgNPs

According to existing research, the major processes underlying the antibacterial effects of NPs, under *in vivo* conditions are: (1) Penetration and disruption of the bacterial cell membrane due to very small size; (2) release of Ag<sup>+</sup> ions; (3) generation of ROS that inhibits the antioxidant defense system and damages vital components inside the cell; and (4) induction of intracellular antibacterial effects, including interactions with DNA and proteins (Fig. 9). This multifaceted approach may make it more difficult for microbes to develop resistance.

**Table 3: Antibacterial activity of AgNPs and synergistic activity with streptomycin against pathogenic bacteria (data shown in ZOI [in mm])**

Bacteria	Streptomycin (10 µg/ml)	Single concentration of AgNPs 200 µg/ml	AgNPs 100 µg/ml + streptomycin	AgNPs 150 µg/ml + Streptomycin	AgNPs 200 µg/ml + Streptomycin
<i>P. aeruginosa</i> MTCC 424	11.03±0.03	12.09±0.01	13.01±0.04	13.08±0.11	14.03±0.83
<i>E. coli</i> MTCC 40	10.07±0.94	11.59±0.55	11.76±0.04	11.84±0.02	11.94±0.04
<i>P. mirabilis</i> MTCC 3310	10.88±0.10	12.58±1.19	13.60±0.01	14.08±0.03	15.30±0.03
<i>S. aureus</i> MTCC 9760	11.07±0.00	11.98±0.00	13.00±0.06	14.50±0.02	14.01±0.48
<i>S. pyogenes</i> MTCC 1926	11.09±2.17	11.12±0.10	11.23±0.00	11.38±0.12	11.54±0.03
<i>B. cereus</i> MTCC 430	11.03±0.04	11.15±0.03	11.20±0.05	11.45±0.17	11.64±0.03

AgNPs: Silver nanoparticles, ZOI: Zone of inhibition, *S. aureus*: *Staphylococcus aureus*, *S. pyogenes*: *Streptococcus pyogenes*, *P. mirabilis*: *Proteus mirabilis*, *P. aeruginosa*: *Pseudomonas aeruginosa*

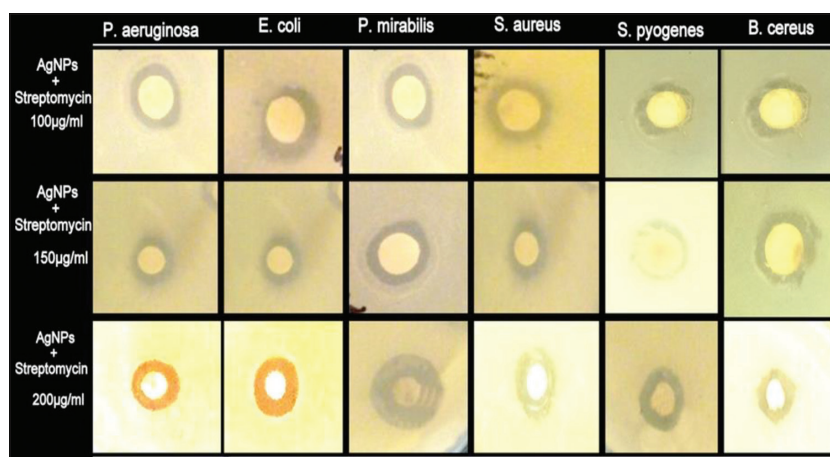


**Fig. 8: Antibacterial activity of silver nanoparticles (AgNPs) at 100, 150, and 200 µg/ml and synergistic antibacterial potential of AgNPs with standard antibiotics, streptomycin (10 µg/ml) by measuring ZOI**

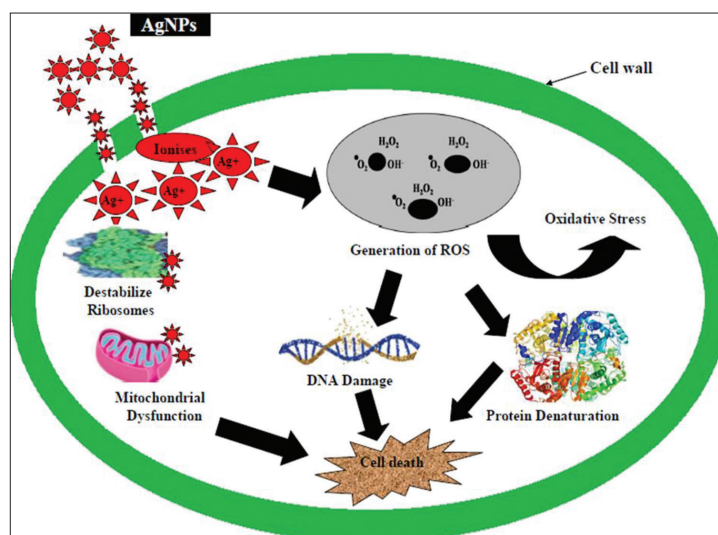


**Fig. 9: Hypothetical model representing mechanism of antibacterial action of silver nanoparticles**

The potential advantage of nanoparticles is that they directly destroy bacterial membranes without targeting a very specific step in their metabolic pathways, as do most traditional antibiotics. This may be responsible for the suppressed resistance to nanoparticles [33].

## CONCLUSION

In this study, AgNPs were green synthesized from *C. roseus* leaf extract at pH 5, temp 80°C, and concentration of 1 mM kept for 72 h. The high alkaloid content of *C. roseus* leaf extract has strong reductive properties which assisted in the reduction of Ag<sup>+</sup> ions to AgNPs. The shape of nanoparticles was found to be spherical. The size of nanoparticles was measured to be about 60 nm by SEM, DLS, and AFM. Optimum conditions were obtained (pH, temp, concentration, and incubation period) for getting the best attributes of AgNPs such as very smaller size, morphology (spherical), purity, higher amount of Ag, uniform distribution (monodispersity), and crystalline structure. These features contribute to a high antibacterial efficacy (especially in synergy with an antibiotic) against all six tested pathogens as revealed by ZOI method.

## Future prospects

Synthesis of AgNPs through biological route (*C. roseus* leaf extract) is an economical, rapid, and non-hazardous method that can help in their commercial production on a large scale. This study provides an insight to regulation of properties of nanoparticles which would make them efficient in multi-faceted uses such as in pharmaceuticals, drug delivery, therapeutics, cosmetics, nanoelectronics, plastics, and agriculture.

Researches in future should explore AgNPs as potential antimicrobial agent for wide spectrum of other infectious microorganisms. The combination of AgNPs with antibiotics will provide a novel path to develop new compounds to win battle against multi-drug resistant pathogens. This synergistic effect will also reduce the dependency on synthetic drugs and patients can be given more effective treatment and reduce the pain from traditional methods of treatment.

## ACKNOWLEDGMENT

We wish to express our sincere acknowledgment to Dr. Ashok Kumar Chauhan, President, RBEF parent organization of Amity University Madhya Pradesh (AUMP), Dr. Aseem Chauhan, Additional President, RBEF and chairman of Amity University Gwalior Campus, Lt. Gen. V.K. Sharma, AVSM (Retd.), Vice Chancellor of AUMP Gwalior Campus, for providing necessary facilities, their valuable support and encouragement throughout the work.

## AUTHORS' CONTRIBUTIONS

MG performed all the experiments and wrote the manuscript draft and design the concept and finalized the manuscript.

## CONFLICTS OF INTEREST

The authors confirm that they have no conflicts of interest.

## Data availability statement in your manuscript

All the raw data available.

## Funding statement

No funding available. AUMP Gwalior provided the money for research work.

## REFERENCES

- Bharali DJ, Sahoo SK, Mozumdar S, Maitra A. Cross-linked polyvinylpyrrolidone nanoparticles: A potential carrier for hydrophilic drugs. *J Colloid Interface Sci* 2003;258:415-23.
- Ibrahim HM. Green synthesis and characterization of silver nanoparticles using banana peel extract and their antimicrobial activity against representative microorganisms. *J Radiat Res Appl Sci* 2015;8:265-75.
- Ahmed S, Ullah S, Swami BL, Ikram S. Green synthesis of silver nanoparticles using *Azadirachta indica* aqueous leaf extract. *J Radiat Res Appl Sci* 2016;9:1-7.
- Xia ZK, Ma QH, Li SY, Zhang DQ, Cong L, Tian YL, *et al.* The antifungal effect of silver nanoparticles on *Trichosporon asahii*. *J Microbiol Immunol Infect* 2016;49:182-8.
- Le Ouay B, Stellacci F. Antibacterial activity of silver nanoparticles: A surface science insight. *Nanotoday* 2015;10:339-54.
- Kumar B, Smita K, Cumbal L. Biosynthesis of silver nanoparticles using lavender leaf and their applications for catalytic, sensing, and antioxidant activities. *Nanotechnol Rev* 2016;5:521-8.
- El-Rafie HM, Hamed AA. Antioxidant and anti-inflammatory activities of silver nanoparticles biosynthesized from aqueous leaves extracts of four *Terminalia* species. *Adv Nat Sci Nanosci Nanotechnol* 2014;5:035008.
- Garg S, Chandra A, Mazumder A, Mazumder R. Green synthesis of silver nanoparticles using *Arnebia nobilis* root extract and wound healing potential of its hydrogel. *Asian J Pharm* 2014;8:95-101.
- Singh H, Du J, Singh P, Yi TH. Ecofriendly synthesis of silver and gold nanoparticles by *Euphrasia officinalis* leaf extract and its biomedical applications. *Artif Cells Nanomed Biotechnol* 2018;46:1163-70.
- Saha M, Bandyopadhyay PK. Green biosynthesis of silver nanoparticle using garlic, *Allium sativum* with reference to its antimicrobial activity against the pathogenic strain of *Bacillus sp.* and *Pseudomonas sp.* infecting goldfish, *Carassius auratus*. *Proc Zool Soc* 2019;72:180-6.
- Moodley JS, Krishna SB, Pillay K, Govender P. Green synthesis of silver nanoparticles from *Moringa oleifera* leaf extracts and its antimicrobial potential. *Adv Nat Sci Nanosci Nanotechnol* 2018;9:015011.
- Gupta M, Tomar RS, Mishra RK. Factors affecting biosynthesis of green nanoparticles. *Our Heritage* 2020;68:10535-55.
- Gupta M, Tomar RS, Kaushik S, Sharma D, Mishra RK. Effective antimicrobial activity of green ZnO nano particles of *Catharanthus roseus*. *Front Microbiol* 2018;9:2030.
- Chen Y, Ding H, Sun S. Preparation and characterization of ZnO nanoparticles supported on amorphous SiO<sub>2</sub>. *Nanomaterials (Basel)* 2017;7:217.
- Roopan SM, Madhumitha G, Rahuman AA, Kamaraj C, Bharathi A, Surendra TV. Low-cost and eco-friendly phyto-synthesis of silver nanoparticles using *Cocos nucifera* coir extract and its larvicidal activity. *Ind Crops Prod* 2013;43:631-5.
- Prasad TN, Elumalai EK. Biofabrication of Ag nanoparticles using *Moringa oleifera* leaf extract and their antimicrobial activity. *Asian Pac J Trop Biomed* 2011;1:439-42.
- Vanaja M, Gnanajobitha G, Paulkumar K, Rajeshkumar S, Malarkodi C, Annadurai G. Phytosynthesis of silver nanoparticles by *Cissus quadrangularis*: Influence of physicochemical factors. *J Nanostruct Chem* 2013;3:17.
- Bar H, Bhui DK, Sahoo GP, Sarkar P, De SP, Misra A. Green synthesis of silver nanoparticles using latex of *Jatropha curcas*. *Colloids Surf A Physicochem Eng Asp* 2009;339:134-9.
- Anandalakshmi K, Venugobal J. Green synthesis and characterization of silver nanoparticles using *Vitex negundo* (Karu Nochchi) leaf extract and its antibacterial activity. *Med Chem (Los Angeles)* 2017;7:218-25.
- Valsalam S, Agastian P, Arasu MV, Al-Dhabi NA, Ghilan AK, Kaviyarasu K, *et al.* Rapid biosynthesis and characterization of silver nanoparticles from the leaf extract of *Tropaeolum majus* L. and its enhanced *in-vitro* antibacterial, antifungal, antioxidant and anticancer properties. *J Photochem Photobiol B* 2019;191:65-74.
- Rashid MI, Mujawar LH, Rehan ZA, Qari H, Zeb J, Almeelbi T, *et al.* One-step synthesis of silver nanoparticles using *Phoenix dactylifera* leaves extract and their enhanced bactericidal activity. *J Mol Liq* 2016;223:1114-22.
- Ajayi E, Afolayan A. Green synthesis, characterization and biological activities of silver nanoparticles from alkalized *Cymbopogon citratus* *Stapf*. *Adv Nat Sci Nanosci Nanotechnol* 2017;8:015017.
- Tippayawat P, Phromviyo N, Boueroy P, Chompoosor A. Green synthesis of silver nanoparticles in *Aloe vera* plant extract prepared by a hydrothermal method and their synergistic antibacterial activity. *PeerJ* 2016;4:e2589.
- Hebeish A, El-Rafie MH, El-Sheikh MA, El-Naggar ME. Nanostructural features of silver nanoparticles powder synthesized through concurrent formation of the nanosized particles of both starch and silver. *J Nanotechnol* 2013;2013:201057.
- Vigneshwaran N, Bijukumar G, Karmakar N, Anand S, Misra A. Autofluorescence characterization of advanced glycation end products of hemoglobin. *Spectrochim Acta A Mol Biomol Spectrosc* 2005;61:163-70.
- Logeswari P, Silambarasan S, Abraham J. Synthesis of silver

- nanoparticles using plants extract and analysis of their antimicrobial property. J Saudi Chem Soc 2015;19:311-7.
27. Aruna A, Karthikeyan V, Bose P. Synthesis and characterization of silver nanoparticles of insulin plant (*Costus pictus* D. Don) leaves. Asian J Biomed Pharm Sci 2014;4:1-6.
  28. Bhau BS, Ghosh S, Puri S, Borah B, Sarmah DK, Khan R. Green synthesis of gold nanoparticles from the leaf extract of *Nepenthes khasiana* and antimicrobial assay. Adv Mater Lett 2015;6:55-8.
  29. Shaik MR, Ali ZJ, Khan M, Kuniyil M, Assal ME, Alkathlan HZ, *et al.* Green synthesis and characterization of palladium nanoparticles using *Origanum vulgare* L. extract and their catalytic activity. Molecules 2017;22:165.
  30. Kumar B, Smita K, Cumbal L, Debut A. *Ficus carica* (Fig) fruit mediated green synthesis of silver nanoparticles and its antioxidant activity: A comparison of thermal and ultrasonication approach. Bionanoscience 2016;6:15-21.
  31. Valli JS, Vaseeharan B. Biosynthesis of silver nanoparticles by *Cissus quadrangularis* extracts. Mater Lett 2012;82:171-3.
  32. Anandalakshmi K, Venugobal J, Ramasamy V. Characterization of silver nanoparticles by green synthesis method using *Petalium murex* leaf extract and their antibacterial activity. Appl Nanosci 2016;6:399-408.
  33. Sondi I, Salopek-Sondi B. Silver nanoparticles as antimicrobial agent: A case study on *E. coli* as a model for Gram-negative bacteria. J Colloid Interface Sci 2004;275:177-82.